Influence of the hadronic equation of state on the hadron-quark phase transition in neutron stars

F. Yang and H. Shen*
Department of Physics, Nankai University, Tianjin 300071, People's Republic of China
(Received 18 September 2007; published 11 February 2008)

We study the hadron-quark phase transition in the interior of neutron stars. The relativistic mean field (RMF) theory is adopted to describe the hadronic matter phase, while the Nambu-Jona-Lasinio (NJL) model is used for the quark matter phase. The influence of the hadronic equation of state on the phase transition and neutron star properties are investigated. We find that a neutron star possesses a large population of hyperons, but it is not dense enough to possess a pure quark core. Whether the mixed phase of hadronic and quark matter exist in the core of neutron stars depends on the RMF parameters used.

DOI: 10.1103/PhysRevC.77.025801 PACS number(s): 26.60.Kp, 24.10.Jv, 24.85.+p, 97.60.Jd

I. INTRODUCTION

Neutron stars are laboratories for dense matter physics, since they contain matter in one of the densest forms found in the universe. It is expected that the deconfinement phase transition may occur in the core of massive neutron stars [1]. The study of the hadron-quark phase transition at high density is of great interest in both nuclear physics and astrophysics. It has been pointed out by Glendenning [2] that the hadron-quark phase transition in neutron stars may proceed through a mixed phase of hadronic and quark matter over a finite range of pressures and densities according to the Gibbs criteria for phase equilibrium. Such phase transition has received much attention in neutron star physics [3–11]. It is believed that hyperons may appear around twice normal nuclear matter density through the weak interaction [12], which usually occur earlier than the hadron-quark phase transition. The inclusion of hyperons in the hadronic phase alters the threshold density and properties of the mixed phase significantly. In general, the presence of new degrees of freedom, such as hyperons and quarks, tends to soften the equation of state (EOS) at high density and lower the maximum mass of neutron stars.

To study the hadron-quark phase transition, we need models to describe hadronic matter and quark matter. Unfortunately, there is no single model which can be used to describe both phases and the dynamic process of the phase transition. We have to use different approaches for the description of the two phases, then perform the Glendenning construction for the charge-neutral mixed phase where both hadronic and quark phases coexist [2]. In this work, we adopt the relativistic mean field (RMF) theory to describe the hadronic matter phase, while the Nambu-Jona-Lasinio (NJL) model is used for the quark matter phase. The choice of the NJL model is motivated by the fact that this model can successfully reproduce many aspects of quantum chromodynamics such as the nonperturbative vacuum structure and dynamical breaking of chiral symmetry [13–15]. We adopt a three-flavor version of the NJL model to describe the quark matter phase [13]. With a definite EOS for quark matter based on the NJL model, we examine the influence of the hadronic EOS on the hadron-quark phase transition and neutron star properties.

We use the RMF theory to describe the hadronic matter phase. The RMF theory has been successfully and widely used for the description of nuclear matter and finite nuclei [16–20]. It has also been applied to provide the EOS of dense matter for the use in supernovae and neutron stars [21,22]. In the RMF approach, baryons interact through the exchange of scalar and vector mesons. The meson-nucleon coupling constants are generally determined by fitting to some nuclear matter properties or ground-state properties of finite nuclei. However, there are large uncertainties in the meson-hyperon couplings due to limited experimental data. One can use the coupling constants derived from the quark model, or those values constrained by reasonable hyperon potentials. The two additional strange mesons, σ^* and ϕ, were originally introduced in order to obtain the strong attractive hyperon-hyperon (YY) interaction deduced from the earlier measurement [23]. A recent observation of the double-Λ hypernucleus ${}^{\ 6}_{\Lambda\Lambda}\mathrm{He}$, called the Nagara event [24], has had a significant impact on strangeness nuclear physics. The Nagara event provides unambiguous identification of ${}^{\ 6}_{\Lambda\Lambda}\mathrm{He}$ production with precise $\Lambda\Lambda$ binding energy value $B_{\Lambda\Lambda} = 7.25 \pm 0.19^{+0.18}_{-0.11}$ MeV, which suggests that the effective $\Lambda\Lambda$ interaction should be considerably weaker ($\triangle B_{\Lambda\Lambda} \sim 1$ MeV) than that deduced from the earlier measurement ($\triangle B_{\Lambda\Lambda} \sim 5$ MeV). The weak YY interaction suggested by the Nagara event has been used to reinvestigate the properties of multistrange systems, and it has been found that the change of YY interactions affects the properties of strange hadronic matter dramatically [25–27]. In order to examine the influence of the hadronic EOS on the hadron-quark phase transition, we employ two successful parameter sets of the RMF model, NL3 [28] and TM1 [29], which have been widely used for the description of nuclear matter and finite nuclei including unstable nuclei. For each parameter set of the nucleonic sector, we consider two cases of hyperon-hyperon interactions, the weak and strong YY interactions. By comparing the results with different parametrizations in the RMF model, we evaluate how sensitive the hadron-quark phase transition is to the hadronic EOS used in the calculation.

For a comprehensive description of neutron stars, we need not only the EOS at high density for the interior region but

*songtc@nankai.edu.cn

 ©2008 The American Physical Society

also the EOS for the inner and outer crusts, where the density is low and heavy nuclei exist. For the nonuniform matter at low density, we adopt a relativistic EOS based on the RMF theory with a local density approximation [21,22]. The nonuniform matter is modelled to be composed of a lattice of spherical nuclei immersed in an electron gas with or without free neutrons dripping out of nuclei. As the density increases, heavy nuclei dissolve and the optimal state is a uniform matter consisting of neutrons, protons, and leptons (electrons and muons) in β equilibrium. The low density EOS is therefore matched to an EOS of uniform nuclear matter at around 10^{14} g/cm^3 [22]. At higher densities, some additional degrees of freedom such as hyperons and quarks may occur, and the hadron-quark phase transition could proceed through a mixed phase of hadronic and quark matter [5–11]. Applying the EOS of neutron star matter over a wide density range, we study the neutron star properties by solving the Tolman-Oppenheimer-Volkoff equation, and examine whether or not the deconfined quark phase can exist in the core of neutron stars.

This paper is arranged as follows. In Sec. II, we discuss the EOS for hadronic matter in the RMF theory, and the parameters used in the calculation. In Sec. III, the NJL model is used for the description of quark matter. In Sec. IV, we investigate the hadron-quark phase transition of neutron star matter, and examine the influence of the hadronic EOS. We present in Sec. V the properties of neutron stars. Section VI is devoted to a summary.

II. HADRONIC PHASE

To describe the hadronic matter phase, we adopt the relativistic mean field (RMF) theory, in which baryons interact via the exchange of mesons. The baryons considered in this work are nucleons (p and n) and hyperons (Λ, Σ, and Ξ). The exchanged mesons include isoscalar scalar and vector mesons (σ and ω), isovector vector meson (ρ), and two additional hidden-strangeness mesons (σ^* and ϕ). For neutron star matter consisting of a neutral mixture of baryons and leptons in β equilibrium, we start from the effective Lagrangian

$$\begin{aligned}\mathcal{L}_{\rm RMF} = &\sum_B \bar{\psi}_B \left[i\gamma_\mu \partial^\mu - m_B - g_{\sigma B}\sigma - g_{\sigma^* B}\sigma^* \right.\\ &\left. - g_{\omega B}\gamma_\mu \omega^\mu - g_{\phi B}\gamma_\mu \phi^\mu - g_{\rho B}\gamma_\mu \tau_i \rho_i^\mu \right] \psi_B\\ &+ \frac{1}{2}\partial_\mu\sigma\,\partial^\mu\sigma - \frac{1}{2}m_\sigma^2\sigma^2 - \frac{1}{3}g_2\sigma^3 - \frac{1}{4}g_3\sigma^4\\ &- \frac{1}{4}W_{\mu\nu}W^{\mu\nu} + \frac{1}{2}m_\omega^2\omega_\mu\omega^\mu + \frac{1}{4}c_3(\omega_\mu\omega^\mu)^2\\ &- \frac{1}{4}R_{i\mu\nu}R_i^{\mu\nu} + \frac{1}{2}m_\rho^2\rho_{i\mu}\rho_i^\mu + \frac{1}{2}\partial_\mu\sigma^*\partial^\mu\sigma^*\\ &- \frac{1}{2}m_{\sigma^*}^2\sigma^{*2} - \frac{1}{4}S_{\mu\nu}S^{\mu\nu} + \frac{1}{2}m_\phi^2\phi_\mu\phi^\mu\\ &+ \sum_l \bar{\psi}_l[i\gamma_\mu\partial^\mu - m_l]\psi_l, \end{aligned} \tag{1}$$

where the sum on B runs over the baryon octet (p, n, Λ, Σ^+, Σ^0, Σ^-, Ξ^0, Ξ^-), and the sum on l is over electrons and muons (e^- and μ^-). In the RMF model, the meson fields are treated as classical fields, and the field operators are replaced by their expectation values. The meson field equations in uniform matter have the following form:

$$m_\sigma^2\sigma + g_2\sigma^2 + g_3\sigma^3 = -\sum_B \frac{g_{\sigma B}}{\pi^2}\int_0^{k_F^B} \frac{m_B^*}{\sqrt{k^2+m_B^{*2}}}k^2dk, \tag{2}$$

$$m_\omega^2\omega + c_3\omega^3 = \sum_B \frac{g_{\omega B}\left(k_F^B\right)^3}{3\pi^2}, \tag{3}$$

$$m_\rho^2\rho = \sum_B \frac{g_{\rho B}\tau_{3B}\left(k_F^B\right)^3}{3\pi^2}, \tag{4}$$

$$m_{\sigma^*}^2\sigma^* = -\sum_B \frac{g_{\sigma^* B}}{\pi^2}\int_0^{k_F^B} \frac{m_B^*}{\sqrt{k^2+m_B^{*2}}}k^2dk, \tag{5}$$

$$m_\phi^2\phi = \sum_B \frac{g_{\phi B}\left(k_F^B\right)^3}{3\pi^2}, \tag{6}$$

where $\sigma = \langle\sigma\rangle$, $\omega = \langle\omega^0\rangle$, $\rho = \langle\rho^{30}\rangle$, $\sigma^* = \langle\sigma^*\rangle$, and $\phi = \langle\phi^0\rangle$ are the nonvanishing expectation values of meson fields in neutron star matter. $m_B^* = m_B + g_{\sigma B}\sigma + g_{\sigma^* B}\sigma^*$ is the effective mass of the baryon species B, and k_F^B is the Fermi momentum.

In this work, we employ two successful parameter sets of the RMF model, NL3 and TM1, as listed in Table I. These parameters have been determined by fitting to some ground-state properties of finite nuclei, and they can provide good description of nuclear matter and finite nuclei including unstable nuclei [28,29]. As for the meson-hyperon couplings, we take the naive quark model values for the vector coupling constants,

$$\begin{aligned}&\frac{1}{3}g_{\omega N} = \frac{1}{2}g_{\omega\Lambda} = \frac{1}{2}g_{\omega\Sigma} = g_{\omega\Xi},\\ &g_{\rho N} = \frac{1}{2}g_{\rho\Sigma} = g_{\rho\Xi}, \quad g_{\rho\Lambda} = 0,\\ &2g_{\phi\Lambda} = 2g_{\phi\Sigma} = g_{\phi\Xi} = -\frac{2\sqrt{2}}{3}g_{\omega N}, \quad g_{\phi N} = 0.\end{aligned} \tag{7}$$

TABLE I. The parameter sets NL3 [28] and TM1 [29] used in the calculation. The masses are given in MeV.

	m_N	m_σ	m_ω	m_ρ	$g_{\sigma N}$	$g_{\omega N}$	$g_{\rho N}$	g_2 (fm^{-1})	g_3	c_3
NL3	939.0	508.194	782.501	763.0	10.217	12.868	4.474	−10.431	−28.885	–
TM1	938.0	511.198	783.0	770.0	10.029	12.614	4.632	−7.233	0.618	71.308

TABLE II. The scalar coupling constants for the hyperons.

	$g_{\sigma\Lambda}$	$g_{\sigma\Sigma}$	$g_{\sigma\Xi}$	$g_{\sigma^*\Lambda(\Sigma)}$	$g_{\sigma^*\Xi}$
NL3 (weak YY)	6.269	4.709	3.242	5.595	11.765
NL3 (strong YY)	6.269	4.709	3.242	7.138	12.809
TM1 (weak YY)	6.170	4.472	3.202	5.412	11.516
TM1 (strong YY)	6.170	4.472	3.202	7.018	12.600

The scalar coupling constants are chosen to give reasonable hyperon potentials. The potential depth of the hyperon species i in matter of the baryon species j is denoted by $U_i^{(j)}$, and we use $U_\Lambda^{(N)} = -28$ MeV, $U_\Sigma^{(N)} = +30$ MeV, and $U_\Xi^{(N)} = -18$ MeV [30–32] to determine the scalar coupling constants $g_{\sigma\Lambda}$, $g_{\sigma\Sigma}$, and $g_{\sigma\Xi}$, respectively. The hyperon couplings to strange meson σ^* are restricted by the relation $U_\Xi^{(\Xi)} \simeq U_\Lambda^{(\Xi)} \simeq 2U_\Xi^{(\Lambda)} \simeq 2U_\Lambda^{(\Lambda)}$ obtained in Ref. [33]. We consider two cases of hyperon-hyperon (YY) interactions. The strong YY interaction deduced from the earlier measurement [23] suggests $U_\Lambda^{(\Lambda)} \simeq -20$ MeV, while the weak YY interaction implied by the Nagara event suggests $U_\Lambda^{(\Lambda)} \simeq -5$ MeV [25–27]. In Table II, we present the meson-hyperon couplings determined by these hyperon potentials. The hyperon masses are taken to be $m_\Lambda = 1115.7$ MeV, $m_\Sigma = 1193.1$ MeV, and $m_\Xi = 1318.1$ MeV, while the strange meson masses are $m_{\sigma^*} = 975$ MeV and $m_\phi = 1020$ MeV.

For neutron star matter consisting of a neutral mixture of baryons and leptons, the β equilibrium conditions without trapped neutrinos are given by

$$\mu_p = \mu_{\Sigma^+} = \mu_n - \mu_e, \tag{8}$$

$$\mu_\Lambda = \mu_{\Sigma^0} = \mu_{\Xi^0} = \mu_n, \tag{9}$$

$$\mu_{\Sigma^-} = \mu_{\Xi^-} = \mu_n + \mu_e, \tag{10}$$

$$\mu_\mu = \mu_e, \tag{11}$$

where μ_i is the chemical potential of species i. At zero temperature the chemical potentials of baryons and leptons are expressed by

$$\mu_B = \sqrt{k_F^{B\,2} + m_B^{*2}} + g_{\omega B}\omega + g_{\phi B}\phi + g_{\rho B}\tau_{3B}\rho, \tag{12}$$

$$\mu_l = \sqrt{k_F^{l\,2} + m_l^2}. \tag{13}$$

The charge neutrality condition is given by

$$n_p + n_{\Sigma^+} = n_e + n_\mu + n_{\Sigma^-} + n_{\Xi^-}, \tag{14}$$

where $n_i = (k_F^i)^3/(3\pi^2)$ is the number density of species i. We can solve the coupled equations self-consistently at a given baryon density $n_B = n_p + n_n + n_\Lambda + n_{\Sigma^+} + n_{\Sigma^0} + n_{\Sigma^-} + n_{\Xi^0} + n_{\Xi^-}$. The total energy density and pressure of neutron star matter are written by

$$\begin{aligned}\varepsilon_{\rm HP} = {} & \sum_B \frac{1}{\pi^2}\int_0^{k_F^B} \sqrt{k^2 + m_B^{*2}}\,k^2 dk + \frac{1}{2}m_\sigma^2\sigma^2 + \frac{1}{3}g_2\sigma^3 \\ & + \frac{1}{4}g_3\sigma^4 + \frac{1}{2}m_\omega^2\omega^2 + \frac{3}{4}c_3\omega^4 + \frac{1}{2}m_\rho^2\rho^2 + \frac{1}{2}m_{\sigma^*}^2\sigma^{*2} \\ & + \frac{1}{2}m_\phi^2\phi^2 + \sum_l \frac{1}{\pi^2}\int_0^{k_F^l} \sqrt{k^2 + m_l^2}\,k^2 dk,\end{aligned} \tag{15}$$

$$\begin{aligned}P_{\rm HP} = {} & \frac{1}{3}\sum_B \frac{1}{\pi^2}\int_0^{k_F^B} \frac{k^4 dk}{\sqrt{k^2 + m_B^{*2}}} - \frac{1}{2}m_\sigma^2\sigma^2 - \frac{1}{3}g_2\sigma^3 \\ & - \frac{1}{4}g_3\sigma^4 + \frac{1}{2}m_\omega^2\omega^2 + \frac{1}{4}c_3\omega^4 + \frac{1}{2}m_\rho^2\rho^2 - \frac{1}{2}m_{\sigma^*}^2\sigma^{*2} \\ & + \frac{1}{2}m_\phi^2\phi^2 + \frac{1}{3}\sum_l \frac{1}{\pi^2}\int_0^{k_F^l} \frac{k^4 dk}{\sqrt{k^2 + m_l^2}}.\end{aligned} \tag{16}$$

III. QUARK PHASE

In this section, we adopt a three-flavor version of the NJL model to describe the deconfined quark phase. The Lagrangian is given by

$$\begin{aligned}\mathcal{L}_{\rm NJL} = {} & \bar{q}(i\gamma_\mu\partial^\mu - m^0)q + G\sum_{a=0}^{8}[(\bar{q}\lambda_a q)^2 + (\bar{q}i\gamma_5\lambda_a q)^2] \\ & - K\{\det[\bar{q}(1+\gamma_5)q] + \det[\bar{q}(1-\gamma_5)q]\},\end{aligned} \tag{17}$$

where q denotes a quark field with three flavors ($N_f = 3$) and three colors ($N_c = 3$). $m^0 = \mathrm{diag}(m_u^0, m_d^0, m_s^0)$ is the current quark mass matrix, and we assume isospin symmetry $m_u^0 = m_d^0 \equiv m_q^0$. The coupling constants G and K have dimension energy^{-2} and energy^{-5}, respectively. The model has five parameters, namely, the current quark masses m_q^0 and m_s^0, the coupling constants K and G, and the momentum cutoff Λ. In the present calculation, we employ the parameters given in Ref. [34], $m_q^0 = 5.5$ MeV, $m_s^0 = 140.7$ MeV, $\Lambda = 602.3$ MeV, $G\Lambda^2 = 1.835$, and $K\Lambda^5 = 12.36$. These parameters have been determined by fitting f_π, m_π, m_K, and $m_{\eta'}$ to their empirical values, while the mass of the η-meson is underestimated by about 6% [13].

In the NJL model, the quark gets constituent quark mass by spontaneous chiral symmetry breaking. The constituent quark mass in vacuum m_i is much larger than the current quark mass m_i^0. In the quark matter at high density, the constituent quark mass m_i^* becomes approximately the same as m_i^0, which reflects the restoration of chiral symmetry. Within the mean-field approximation, m_i^* is obtained by solving the gap equation

$$m_i^* = m_i^0 - 4G\langle\bar{q}_i q_i\rangle + 2K\langle\bar{q}_j q_j\rangle\langle\bar{q}_k q_k\rangle, \tag{18}$$

with (i, j, k) being any permutation of (u, d, s). The quark condensate $C_i = \langle\bar{q}_i q_i\rangle$ is given by

$$C_i = -\frac{3}{\pi^2}\int_{k_F^i}^{\Lambda} \frac{m_i^*}{\sqrt{k^2 + m_i^{*2}}}k^2 dk, \tag{19}$$

where k_F^i denotes the Fermi momentum of the quark flavor i, which is connected with the number density n_i and the chemical potential μ_i via

$$n_i = \frac{(k_F^i)^3}{\pi^2}, \tag{20}$$

$$\mu_i = \sqrt{k_F^{i\,2} + m_i^{*2}}. \tag{21}$$

The energy density of the quark system is given by

$$\varepsilon_{\rm NJL} = \sum_{i=u,d,s}\left[-\frac{3}{\pi^2}\int_{k_F^i}^{\Lambda}\sqrt{k^2+m_i^{*2}}k^2dk\right] + 2G\left(C_u^2+C_d^2+C_s^2\right) - 4KC_uC_dC_s - \varepsilon_0, \quad (22)$$

where ε_0 is introduced to ensure $\varepsilon_{\rm NJL} = 0$ in the vacuum.

For the quark matter consisting of a neutral mixture of quarks (u, d, and s) and leptons (e and μ) in β equilibrium, the charge neutrality condition is expressed as

$$\tfrac{2}{3}n_u - \tfrac{1}{3}(n_d+n_s) - n_e - n_\mu = 0, \quad (23)$$

the β equilibrium conditions are given by

$$\mu_s = \mu_d = \mu_u + \mu_e, \quad (24)$$

$$\mu_\mu = \mu_e. \quad (25)$$

The coupled equations can be solved self-consistently at a given baryon density $n_B = (n_u + n_d + n_s)/3$. The total energy density and pressure including the contributions from both quarks and leptons are given by

$$\varepsilon_{\rm QP} = \varepsilon_{\rm NJL} + \sum_{l=e,\mu}\frac{1}{\pi^2}\int_0^{k_F^l}\sqrt{k^2+m_l^2}k^2dk, \quad (26)$$

$$P_{\rm QP} = \sum_{i=u,d,s,e,\mu} n_i\mu_i - \varepsilon_{\rm QP}. \quad (27)$$

IV. HADRON-QUARK PHASE TRANSITION

In this section, we study the hadron-quark phase transition which may occur in the core of massive neutron stars. It has been discussed extensively in the literature that a mixed phase of hadronic and quark matter could exist over a finite range of pressures and densities according to the Gibbs criteria for phase equilibrium. In the mixed phase, the local charge neutrality condition is replaced by a global one. This means that both hadronic and quark matter are allowed to be separately charged. The condition of global charge neutrality is expressed as

$$\chi n_c^{\rm QP} + (1-\chi)n_c^{\rm HP} = 0, \quad (28)$$

where χ is the volume fraction occupied by quark matter in the mixed phase, which increases from $\chi = 0$ in the pure hadronic phase to $\chi = 1$ in the pure quark phase. $n_c^{\rm HP}$ and $n_c^{\rm QP}$ denote the charge densities of hadronic phase and quark phase, respectively. Without the constraint of local charge neutrality, we impose that the two phases are in weak equilibrium and described by two independent chemical potentials (μ_n, μ_e). The Gibbs condition for phase equilibrium at zero temperature is then given by

$$P_{\rm HP}(\mu_n,\mu_e) = P_{\rm QP}(\mu_n,\mu_e). \quad (29)$$

Using Eq. (29) we can calculate the equilibrium chemical potentials of the mixed phase where $P_{\rm HP} = P_{\rm QP} = P_{\rm MP}$ holds. The energy density and the baryon density in the mixed phase are given by

$$\varepsilon_{\rm MP} = \chi\varepsilon_{\rm QP} + (1-\chi)\varepsilon_{\rm HP}, \quad (30)$$

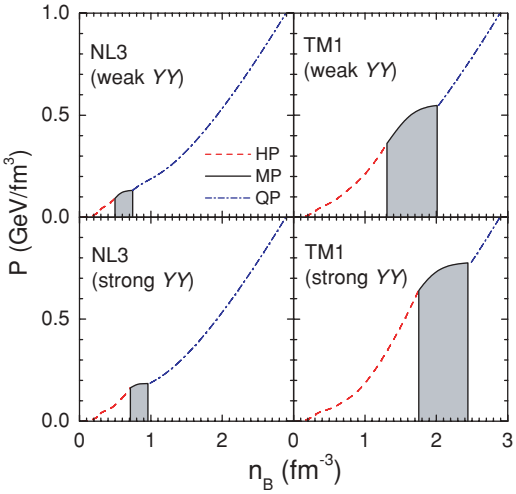

FIG. 1. (Color online) The pressure P as a function of the baryon density n_B. The shaded regions correspond to the mixed phase (MP). The dashed and dot-dashed lines show the pressures of hadronic phase (HP) and quark phase (QP), respectively.

and

$$n_B^{\rm MP} = \chi n_B^{\rm QP} + (1-\chi)n_B^{\rm HP}. \quad (31)$$

We show in Fig. 1 the possible phase structure of neutron star matter using the RMF model for the hadronic phase and the NJL model for the quark phase. To examine the influence of the hadronic EOS on the hadron-quark phase transition, we employ two successful parameter sets of the RMF model, NL3 [28] and TM1 [29], with both the weak and strong YY interactions. The shaded regions correspond to the mixed phase. It is shown that a pure hadronic phase is favored at low density. The mixed phase appears at the critical density $n_B^{(1)}$ where the pressure of the pure hadronic phase becomes to be lower than the pressure of the mixed phase. The fraction of quark matter χ increases with increasing density in the mixed phase. It turns to be a pure quark phase at the critical density $n_B^{(2)}$ where the pressure of the pure quark phase is above the pressure of the mixed phase. The critical densities $n_B^{(1)}$ and $n_B^{(2)}$ are sensitive to the RMF parameters used, and we get $n_B^{(1)} \simeq 0.50$ fm^{-3} (0.71 fm^{-3}) and $n_B^{(2)} \simeq 0.75$ fm^{-3} (0.98 fm^{-3}) for the NL3 parameter set with the weak (strong) YY interaction, while $n_B^{(1)} \simeq 1.31$ fm^{-3} (1.75 fm^{-3}) and $n_B^{(2)} \simeq 2.03$ fm^{-3} (2.49 fm^{-3}) are obtained for the TM1 cases. It is found that the hadron-quark phase transition occurs at lower densities in the NL3 model than in the TM1 model, and in general the weak YY interaction leads to an earlier appearance of the mixed phase. In order to estimate the influence of hadronic EOS on the deconfinement phase transition, we plot in Fig. 2 the hadronic EOS in the different cases and the quark EOS in the NJL model with local charge neutrality as a function of the neutron chemical potential μ_n. The crossing of the hadronic EOS with the quark EOS marks the transition point between the charge neutral hadronic matter and quark matter. It is seen that the NL3 model favors the phase transition at a lower μ_n. A more realistic treatment of the phase transition

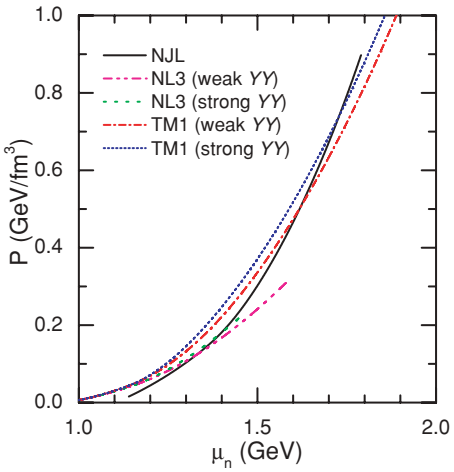

FIG. 2. (Color online) The pressure P as a function of the neutron chemical potential μ_n for hadronic and quark matter with local charge neutrality. The crossing of the hadronic EOS with the quark EOS (NJL) marks the transition point between the charge neutral hadronic matter and quark matter.

is to release the constraint of local charge neutrality, which leads to the existence of the mixed phase of charged hadronic and quark matter over a finite range of pressures and densities as shown in Fig. 1. In general, a harder hadronic EOS also favors an earlier appearance of the mixed phase.

In Fig. 3 we plot the full EOS in the form $P = P(\varepsilon)$, which consists of three parts: (a) the charge neutral hadronic matter phase at low density (b) the mixed phase of charged hadronic and quark matter (c) the charge neutral quark matter phase at high density. The mixed phase part of the EOS is shaded gray, where the pressure varies continuously. It is shown that the onset and width of the mixed phase depend on the RMF parameters used in the calculation. The NL3 model leads to

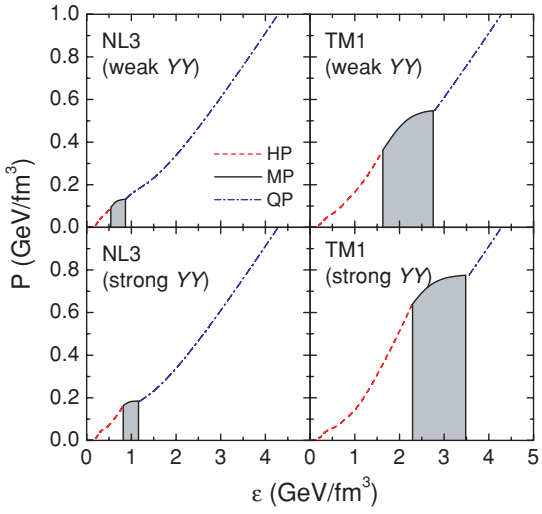

FIG. 3. (Color online) The full EOS of neutron star matter in the form of pressure P versus energy density ε. The shaded regions correspond to the mixed phase (MP). The dashed and dot-dashed lines show the pressures of hadronic phase (HP) and quark phase (QP), respectively.

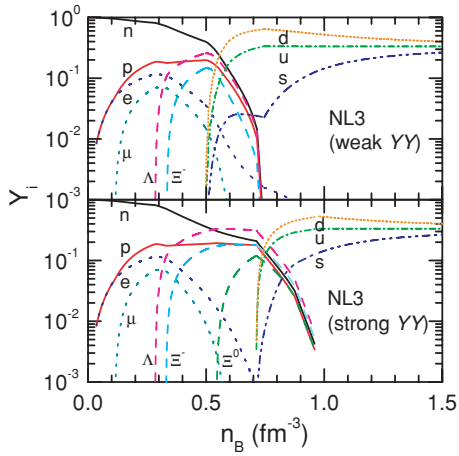

FIG. 4. (Color online) The particle fraction $Y_i = n_i/n_B$ as a function of the total baryon density n_B for the NL3 model.

earlier appearance of the mixed phase than the TM1 model, and the weak YY interaction favors earlier onset of the mixed phase than the strong YY interaction. This is mainly because that a harder hadronic EOS prefers an earlier hadron-quark phase transition. By comparing the results of different cases, we can see the influence of the hadronic EOS on the hadron-quark phase transition.

We present in Figs. 4 and 5 the particle fraction $Y_i = n_i/n_B$ as a function of the total baryon density n_B. At low densities the fractions Y_p, Y_e, andY_μ increase with increasing density. When the Fermi energy of nucleons exceeds the rest mass of hyperons, the conversion of nucleons to hyperons is energetically favorable, and it can relieve the Fermi pressure of nucleons. The fraction of hyperons increases with increasing density before the mixed phase occurs. Quarks appear at the critical density $n_B^{(1)}$, then the fractions Y_u, Y_d, and Y_s increase rapidly with increasing density. The hadronic matter completely disappears at the critical density $n_B^{(2)}$ where the pure quark phase occurs. At extremely high density, $Y_u \sim Y_d \sim Y_s \sim 1/3$ due to the restoration of chiral symmetry. It is

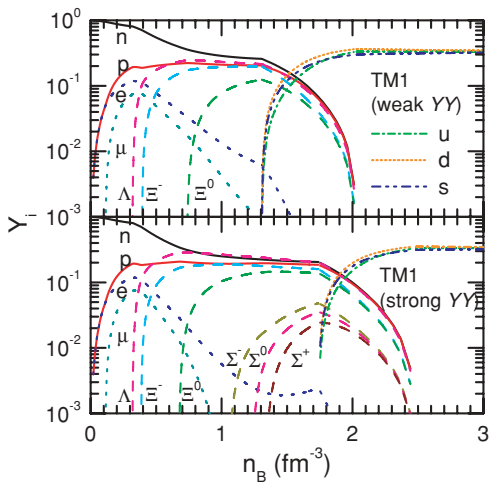

FIG. 5. (Color online) The particle fraction $Y_i = n_i/n_B$ as a function of the total baryon density n_B for the TM1 model.

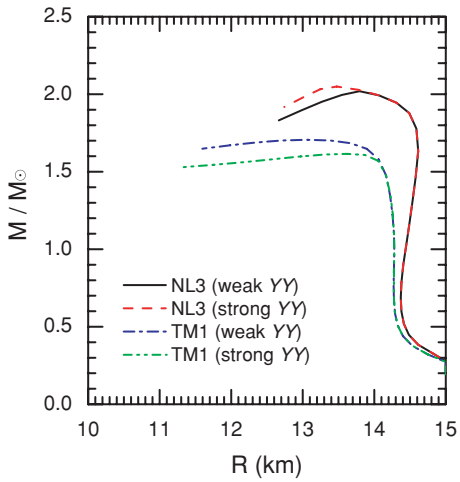

FIG. 6. (Color online) The mass-radius relation for neutron stars.

shown that the composition of neutron star matter depends on the RMF parameters used in the calculation.

V. NEUTRON STARS PROPERTIES

In this section, we investigate the properties of neutron stars by solving the Tolman-Oppenheimer-Volkoff equation with the EOS over a wide density range. For the nonuniform matter at low density, which exists in the inner and outer crusts of neutron stars, we adopt a relativistic EOS based on the RMF theory with a local density approximation [21,22]. The nonuniform matter is modelled to be composed of a lattice of spherical nuclei immersed in an electron gas with or without free neutrons dripping out of nuclei. The low density EOS is matched to the EOS of uniform hadronic matter at the density where they have equal pressures. The pure hadronic phase ends at the critical density $n_B^{(1)}$, and the pure quark phase starts at the critical density $n_B^{(2)}$. The values of these critical densities depend on the RMF parameters used. The neutron star properties are mainly determined by the EOS at high density. We calculate neutron star profiles in order to examine whether or not the deconfined quark phase can exist in the core of neutron stars.

In Fig. 6 we present the mass-radius relation using the EOS of the NL3 and TM1 models with both the weak and strong YY interactions. It is shown that the results depend on the RMF parameters used in the calculation. Since the pressure and density inside neutron stars decrease from the center to the surface, the most possible region where the deconfined quark phase can exist is the center of the neutron star with maximum mass. We list in Table III the properties of neutron stars with the maximum mass. It is found that the central baryon density n_c is between $n_B^{(1)}$ and $n_B^{(2)}$ for the NL3 model. This means that the neutron star can possess a mixed phase core, but it is not dense enough to possess a pure quark core. On the other hand, the values of n_c in the TM1 model are smaller than $n_B^{(1)}$, which means that the neutron star is only composed of hadronic matter. As can be seen in Table III, the neutron star properties significantly depend on the RMF parameters used.

VI. CONCLUSIONS

We have studied the hadron-quark phase transition at high density, which may occur in the core of massive neutron stars. In the present work, we have adopted the RMF theory to describe the hadronic matter phase, while the NJL model has been used for the quark matter phase. With a definite EOS for the quark phase, we examine the influence of the hadronic EOS on the deconfinement phase transition and neutron star properties. In this paper, we employ two successful parameter sets of the RMF model, NL3 and TM1, which have been widely used for the description of nuclear matter and finite nuclei including unstable nuclei. For each parameter set of the nucleonic sector, we consider two cases of hyperon-hyperon interactions, the weak and strong YY interactions. The hadron-quark phase transition can proceed through a mixed phase of hadronic and quark matter over a finite range of pressures and densities according to the Gibbs criteria for phase equilibrium. We have found that the mixed phase starts at $n_B^{(1)} \simeq 0.50$ fm^{-3} (0.71 fm^{-3}) and ends at $n_B^{(2)} \simeq 0.75$ fm^{-3} (0.98 fm^{-3}) for the NL3 parameter set with the weak (strong) YY interaction, while $n_B^{(1)} \simeq 1.31$ fm^{-3} (1.75 fm^{-3}) and $n_B^{(2)} \simeq 2.03$ fm^{-3} (2.49 fm^{-3}) have been obtained for the TM1 cases. It is shown that the hadron-quark phase transition occurs at lower densities in the NL3 model than in the TM1 model, and in general the weak YY interaction leads to an earlier appearance of the mixed phase. By comparing the results with different parametrizations in the RMF model, we can see how sensitive the deconfinement phase transition is to the hadronic EOS used in the calculation.

We have calculated the properties of neutron stars using the EOS over a wide density range. The star properties such as

TABLE III. The properties of neutron stars with the maximum mass $M_{\max}$. The central energy density, pressure, and baryon number density are denoted by ε_c, P_c, and n_c, respectively. R and $R_{\rm MP}$ denote the radii of the star and its mixed phase core.

	$M_{\max}$ ($M_\odot$)	ε_c (10^{15} g/cm^3)	P_c (10^{35} dyn/cm^2)	n_c (fm^{-3})	R (km)	$R_{\rm MP}$ (km)
NL3 (weak YY)	2.02	1.42	2.08	0.69	13.80	4.21
NL3 (strong YY)	2.05	1.46	2.62	0.71	13.48	0.31
TM1 (weak YY)	1.71	1.50	2.08	0.75	13.07	–
TM1 (strong YY)	1.62	1.23	1.32	0.63	13.62	–

their masses and radii are mainly determined by the EOS at high density. We have found the maximum mass of neutron stars falls in the range $1.62 \sim 2.05 M_{\odot}$ for the RMF parameters used. With the NL3 model, the mixed phase can exist in the core of massive neutron stars, but no pure quark phase can exist. For the TM1 model, the neutron star is not dense enough to possess the mixed phase, and therefore the hadron-quark phase transition could not occur inside neutron stars in this approximation. We conclude that the maximum mass and composition of neutron stars depend on the hadronic EOS adopted in the calculation.

It is very interesting to compare our results with those previously published in the literature [5–8]. In Ref. [5], the authors studied the possible hadron-quark phase transition utilizing the same NJL model as used in the present work to describe the deconfined quark phase, while the hadronic phase was described by several RMF models (TM1, TM2, GL85, and GPS as listed in Table I of Ref. [5]). Comparing with our cases, different hyperon potentials were used to constrain the hyperon couplings, but some of their values are not supported by recent experimental observations. They found that the use of the GPS model for the hadronic phase leads to the onset of the mixed phase at the energy density $\epsilon \approx 7\epsilon_0$ ($\epsilon_0 = 140$ MeV/fm^3 is the normal nuclear energy density), while the mixed phase does not appear below $\epsilon \approx 10\epsilon_0$ for the TM1, TM2, and GL85 models. They concluded that within the model constructed in their calculation the appearance of deconfined quark matter in the center of neutron stars turns out to be very unlikely. This is consistent with our results although the hyperon couplings are different between our study and theirs. In Ref. [6], the authors employed an extended MIT bag model to describe the quark phase and four RMF models (TM1, TM2, GL85, and GPS) to describe the hadronic phase. They studied the influence of different hadronic EOS and the influence of the model parameters of the quark phase on the properties of the phase transition. Using the MIT bag model, they found the mixed phase could appear below $\epsilon \approx 2\epsilon_0$, which is much lower than the threshold density obtained using the NJL model. This can be seen by comparing Fig. 4 of Ref. [6] with Fig. 9 of Ref. [5] and Fig. 3 of the present paper. In Ref. [7], the authors investigated the deconfinement phase transition at zero and finite temperature using both the MIT bag model and the NJL model for describing the quark phase and a RMF model (GL model) for the hadronic phase. For the NJL model, however, they adopted another parameter set which favors an earlier onset of the mixed phase than the parameter set used in our calculation. For the hyperon couplings, they used three choices and verified that for the NJL model the onset of the mixed phase is very sensitive to the choice of the hyperon couplings. Using the NJL model for the quark phase, they obtained two different behaviors. One is the hyperons appear before the quarks and the mixed phase occurs at much higher densities ($\sim 5\rho_0$ with the normal nuclear matter density $\rho_0 = 0.153$ fm^{-3}). The other is the quarks appear at lower densities than the hyperons and the mixed phase occurs at $\sim 2\rho_0$. For almost all EOS used in their study, the central energy density of the maximum-mass neutron star falls inside the mixed phase, so the star can contain a core constituted by a mixed phase, but it is not dense enough to possess a pure quark core. In Ref. [8], the authors investigated the deconfinement phase transition using an effective-field-theory-motivated RMF (E-RMF) model for the hadronic phase and considering both unpaired quark matter (UQM) described by the MIT bag model and paired quarks described by the color-flavor locked (CFL) phase for the quark phase. They mentioned that they could not get any mixed phase with the original G2 parameter set in the E-RMF model, so they changed incompressibility K from 215 to 300 MeV and the effective mass m_N^*/m_N from 0.664 to 0.7 to determine a modified parameter set G2* as given in Table I of Ref. [8]. For the hyperon couplings, they assumed that all the hyperons in the octet have the same couplings. Using the G2* parameter set in the E-RMF model for the hadronic phase and $B^{1/4} = 170$ MeV in the UQM model for the quark phase, they obtained the onset of the mixed phase at $\sim 1.3\rho_0$, while the appearance of the mixed phase starts at $\sim 2.4\rho_0$ using the CFL model with $B^{1/4} = 188$ MeV for the quark phase. In our cases, the mixed phase occurs at $\sim 3.3\rho_0$ ($8.6\rho_0$) using the NL3 (TM1) model with the weak YY interaction for the hadronic phase and the NJL model for the quark phase. For simplicity, we have not considered the color-flavor locked phase in the present work. By comparing all these results, we conclude that the deconfinement phase transition is very sensitive to both the hadronic EOS and the quark EOS, whether or not the deconfined quark matter appears in the center of neutron stars depends on the models adopted in the calculation.

ACKNOWLEDGMENTS

This work was supported in part by the National Natural Science Foundation of China (No. 10675064) and the Specialized Research Fund for the Doctoral Program of Higher Education (No. 20040055010).

[1] F. Weber, Prog. Part. Nucl. Phys. **54**, 193 (2005).
[2] N. K. Glendenning, Phys. Rev. D **46**, 1274 (1992).
[3] M. Prakash, I. Bombaci, M. Prakash, P. J. Ellis, J. M. Lattimer, and R. Knorren, Phys. Rep. **280**, 1 (1997).
[4] H. Heiselberg and M. Hjorth-Jensen, Phys. Rep. **328**, 237 (2000).
[5] K. Schertler, S. Leupold, and J. Schaffner-Bielich, Phys. Rev. C **60**, 025801 (1999).
[6] K. Schertler, C. Greiner, J. Schaffner-Bielich, and M. H. Thoma, Nucl. Phys. **A677**, 463 (2000).
[7] D. P. Menezes and C. Providência, Phys. Rev. C **68**, 035804 (2003).
[8] B. K. Sharma, P. K. Panda, and S. K. Patra, Phys. Rev. C **75**, 035808 (2007).
[9] A. W. Steiner, M. Prakash, and J. M. Lattimer, Phys. Lett. **B486**, 239 (2000).
[10] G. F. Burgio, M. Baldo, P. K. Sahu, and H.-J. Schulze, Phys. Rev. C **66**, 025802 (2002).
[11] I. Shovkovy, M. Hanauske, and M. Huang, Phys. Rev. D **67**, 103004 (2003).

[12] J. Schaffner and I. N. Mishustin, Phys. Rev. C **53**, 1416 (1996).
[13] M. Buballa, Phys. Rep. **407**, 205 (2005).
[14] U. Vogl and W. Weise, Prog. Part. Nucl. Phys. **27**, 195 (1991).
[15] T. Hatsuda and T. Kunihiro, Phys. Rep. **247**, 221 (1994).
[16] B. D. Serot and J. D. Walecka, Adv. Nucl. Phys. **16**, 1 (1986).
[17] Y. K. Gambhir, P. Ring, and A. Thimet, Ann. Phys. (NY) **198**, 132 (1990).
[18] D. Hirata, K. Sumiyoshi, B. V. Carlson, H. Toki, and I. Tanihata, Nucl. Phys. **A609**, 131 (1996).
[19] Z. Z. Ren, F. Tai, and D. H. Chen, Phys. Rev. C **66**, 064306 (2002).
[20] H. Shen, F. Yang, and H. Toki, Prog. Theor. Phys. **115**, 325 (2006).
[21] H. Shen, H. Toki, K. Oyamatsu, and K. Sumiyoshi, Nucl. Phys. **A637**, 435 (1998).
[22] H. Shen, Phys. Rev. C **65**, 035802 (2002).
[23] J. Schaffner, C. B. Dover, A. Gal, C. Greiner, and H. Stöcker, Phys. Rev. Lett. **71**, 1328 (1993).
[24] H. Takahashi *et al*., Phys. Rev. Lett. **87**, 212502 (2001).
[25] H. Q. Song, R. K. Su, D. H. Lu, and W. L. Qian, Phys. Rev. C **68**, 055201 (2003).
[26] W. L. Qian, R. K. Su, and H. Q. Song, J. Phys. G **30**, 1893 (2004).
[27] I. Bednarek and R. Manka, J. Phys. G **31**, 1009 (2005).
[28] G. A. Lalazissis, J. König, and P. Ring, Phys. Rev. C **55**, 540 (1997).
[29] Y. Sugahara and H. Toki, Nucl. Phys. **A579**, 557 (1994).
[30] D. J. Millener, C. B. Dover, and A. Gal, Phys. Rev. C **38**, 2700 (1988).
[31] J. Schaffner-Bielich and A. Gal, Phys. Rev. C **62**, 034311 (2000).
[32] J. K. Bunta and S. Gmuca, Phys. Rev. C **70**, 054309 (2004).
[33] J. Schaffner, C. B. Dover, A. Gal, C. Greiner, D. J. Millener, and H. Stocker, Ann. Phys. (NY) **235**, 35 (1994).
[34] P. Rehberg, S. P. Klevansky, and J. Hüfner, Phys. Rev. C **53**, 410 (1996).